

Codoping characteristics of Zn with Mg in GaN

K. S. Kim, M. S. Han, G. M. Yang, C. J. Youn, H. J. Lee et al.

Citation: *Appl. Phys. Lett.* **77**, 1123 (2000); doi: 10.1063/1.1289494

View online: <http://dx.doi.org/10.1063/1.1289494>

View Table of Contents: <http://apl.aip.org/resource/1/APPLAB/v77/i8>

Published by the [American Institute of Physics](#).

Additional information on *Appl. Phys. Lett.*

Journal Homepage: <http://apl.aip.org/>

Journal Information: http://apl.aip.org/about/about_the_journal

Top downloads: http://apl.aip.org/features/most_downloaded

Information for Authors: <http://apl.aip.org/authors>

ADVERTISEMENT



Goodfellow
metals • ceramics • polymers • composites
70,000 products
450 different materials
small quantities fast

www.goodfellowusa.com

Codoping characteristics of Zn with Mg in GaN

K. S. Kim, M. S. Han, G. M. Yang,^{a)} C. J. Youn, and H. J. Lee
*Department of Semiconductor Science & Technology and Semiconductor Physics Research Center,
 Chonbuk National University, Duckjin-Dong, Chonju 561-756, Korea*

H. K. Cho and J. Y. Lee
*Department of Material Science and Engineering, KAIST, 373-1 Kusong-Dong, Yusong-gu, Taejon 305-701,
 Korea*

(Received 10 March 2000; accepted for publication 27 June 2000)

The doping characteristics of Mg–Zn codoped GaN films grown by metalorganic chemical vapor deposition are investigated. By means of the concept of Mg–Zn codoping technique, we have grown *p*-GaN showing a low electrical resistivity (0.72 Ω cm) and a high hole concentration ($8.5 \times 10^{17} \text{ cm}^{-3}$) without structural degradation of the film. It is thought that the codoping of Zn atoms with Mg raises the Mg activation ratio by reducing the hydrogen solubility in *p*-GaN. In addition, the measured specific contact resistance of Mg–Zn codoped GaN film is $5.0 \times 10^{-4} \text{ Ω cm}^2$, which is one order of magnitude lower than that of Mg doped only GaN film ($1.9 \times 10^{-3} \text{ Ω cm}^2$).
 © 2000 American Institute of Physics. [S0003-6951(00)02234-8]

The realization of a high conducting *p*-type GaN contact layer is one of the hot issues in the field of III–V nitrides, because it is a crucial component in achieving current injection laser diodes with a low series resistance and a high external quantum efficiency. The III–V nitrides can be made *p* type by incorporating divalent elements such as Zn, Be, and Mg. However, all of these divalent elements have been known to form deep acceptors, the shallowest being Mg with an activation energy of 160 meV from the valence band. Recently, several growth techniques, such as AlGaIn/GaN short period superlattices with modulation doping^{1,2} and codoping of two different dopant sources have been suggested to achieve a low resistive *p*-GaN layer.^{3–5}

Especially, it has been theoretically³ and experimentally^{4,5} suggested that codoping of *n*-type dopants (e.g., Si, O, etc.) together with *p*-type dopants (e.g., Mg, Be, etc.) in GaN is effective in the fabrication of high-conductivity *p*-type GaN. However, codoping of two different *p*-type dopants in GaN has not been reported. This letter describes the codoping characteristics of *p*-type GaN.

When Zn is the sole dopant, the resulting GaN film becomes highly resistive layer.⁶ It was also reported that the activation energy of Zn (370 meV) is deeper than that of Mg.⁷ However, when Mg and Zn are codoped in GaN, the film shows better electrical and structural properties than Mg-doped only GaN film. In this study, we have studied the codoping characteristics of Zn with Mg. Furthermore, we compare the specific contact resistance of both Mg doped only and Mg–Zn codoped GaN films.

All samples were prepared in a horizontal metalorganic chemical vapor deposition (MOCVD) reactor. The source materials of Ga, N, Mg, and Zn are trimethylgallium, ammonia, biscyclopentadienylmagnesium (Cp₂Mg), and diethylzinc (DEZn), respectively. Mg doped and Mg–Zn codoped GaN overlayers with thicknesses of 1–2 μm were grown in a

H₂ ambient at 1080 °C with various molar flow rates of Cp₂Mg and DEZn. Other growth conditions are the same with those of the unintentionally doped GaN.⁸

In order to investigate Mg–Zn codoping characteristics in GaN, first of all, we studied Mg-doped only GaN films by varying the amount of Cp₂Mg flow rates.⁵ The GaN grown under a Cp₂Mg flow rate of 0.643 μmol/min ([Mg]/[Ga] ratio of 7.6×10^{-3}) exhibited a resistivity of 0.82 Ω cm and a hole concentration of $6 \times 10^{17} \text{ cm}^{-3}$ at room temperature. Electrical conducting characteristics of the grown *p*-GaN films after postgrowth rapid thermal annealing (RTA) in N₂ ambient were measured using the four-point probe van der Pauw technique. A magnetic field of 0.5 T and currents between 10 and 100 μA were applied.

As we change DEZn (under constant Cp₂Mg flow rate of 0.643 μmol/min) and Cp₂Mg (under constant DEZn flow rate of 0.616 nmol/min) molar flow rates, the variations of hole densities and resistivities of Mg–Zn codoped GaN films at room temperature are shown in Fig. 1. Theoretically, the codoping of two different *p*-type dopants in GaN is not helpful to achieve a high conducting *p*-type GaN, because it forms a lot of native defect levels leading to hole compensation.³ In spite of this fact, in our prepared samples, we observed there exist optimum Cp₂Mg flow rate of

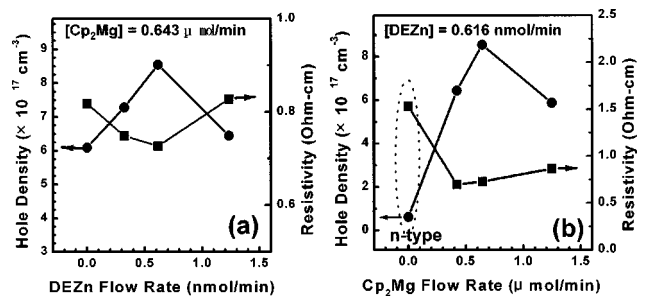


FIG. 1. Dependence of hole densities and resistivities for the Mg–Zn codoped GaN films for (a) various DEZn flow rate and a constant Cp₂Mg flow rate of 0.643 μmol/min and (b) various Cp₂Mg flow rate and constant DEZn flow rate of 0.616 nmol/min.

^{a)} Author to whom correspondence should be addressed; electronic mail: gyemo@moak.chonbuk.ac.kr

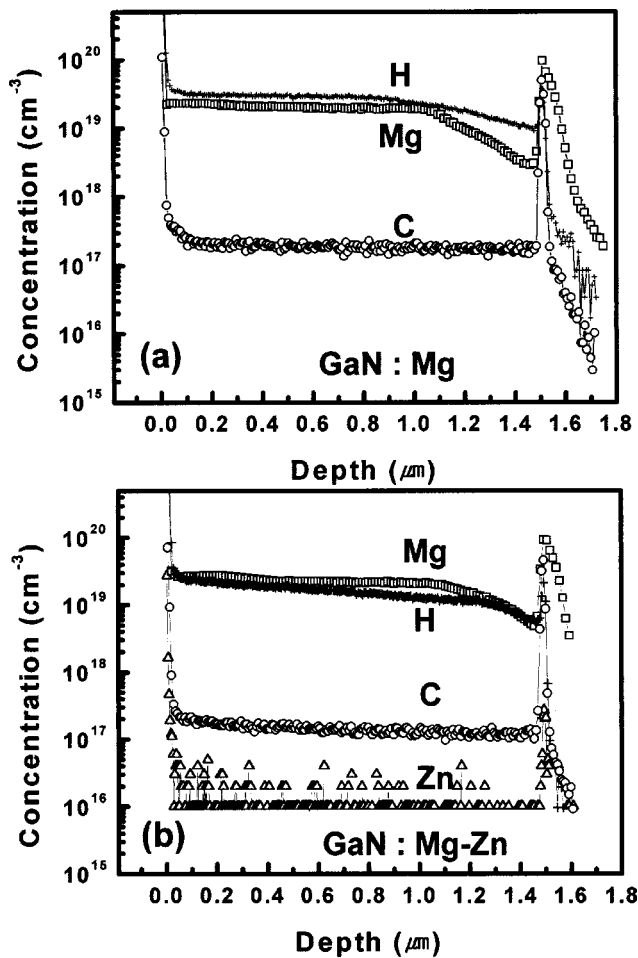


FIG. 2. SIMS depth profiles of (a) Mg-doped only GaN ($[Cp_2Mg] = 0.643 \mu\text{mol/min}$) and (b) Mg-Zn codoped GaN ($[Cp_2Mg] = 0.643 \mu\text{mol/min}$ and $[DEZn] = 0.616 \text{ nmol/min}$). Cross, open square, open circle, and open triangle denote the hydrogen, Mg, carbon, and Zn, respectively.

$0.643 \mu\text{mol/min}$ and DEZn flow rate of 0.616 nmol/min showing the higher hole concentration ($8.5 \times 10^{17} \text{ cm}^{-3}$) and the lower resistivity ($0.72 \Omega \text{ cm}$) than those for Mg-doped only GaN.

For the purpose of accounting for these unexpected results, we measured the depth profiles using secondary ion mass spectroscopy (SIMS) of the as-grown Mg-doped ($6 \times 10^{17} \text{ cm}^{-3}$) only and Mg-Zn codoped ($8.5 \times 10^{17} \text{ cm}^{-3}$) specimens as shown in Fig. 2. Mg and C concentrations are similar without respect to the codoping of Zn, but hydrogen concentration in Mg-doped only GaN is 1.5 times higher than that in Mg-Zn codoped GaN. It is widely accepted that hydrogen incorporated during MOCVD growth behaves as a donor and leads to compensation of acceptors, and a postgrowth annealing step is required to render the acceptor electrically active.⁹ We think that the incorporation of Zn atoms in Mg-doped GaN might reduce the solubility of hydrogen, and thereby it raise the ratio of Mg acceptor activation by RTA. Another interesting fact is that the Zn concentration in Mg-Zn codoped GaN was below our SIMS detection limit of 10^{16} cm^{-3} , even though we observed several photoluminescence peaks corresponding to donor acceptor pair in the Zn-doped (0.616 nmol/min) only GaN (which is not shown here). It is generally known the high vapor

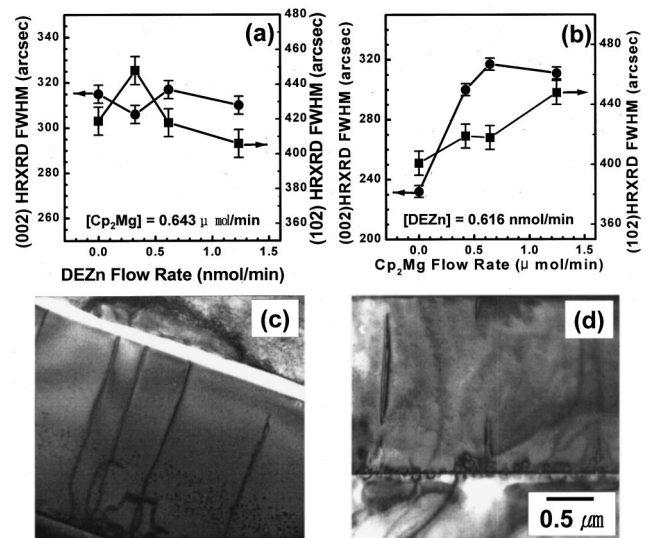


FIG. 3. Dependence of (002) and (102) HRXRD FWHMs for the Mg-Zn codoped GaN films for (a) various DEZn flow rate and a constant Cp_2Mg flow rate of $0.643 \mu\text{mol/min}$ and (b) various Cp_2Mg flow rate and constant DEZn flow rate of 0.616 nmol/min . Cross-sectional (0002) bright-field TEM images of (c) Mg-doped only GaN ($[Cp_2Mg] = 0.643 \mu\text{mol/min}$) and (d) Mg-Zn codoped GaN ($[Cp_2Mg] = 0.643 \mu\text{mol/min}$ and $[DEZn] = 0.616 \text{ nmol/min}$).

pressure of Zn makes Zn unsuited for doping at high temperature. Therefore, at present status, we understand that Zn contributes to the reduction of solubility of hydrogen during the growth at high temperature and mostly desorbs. It should be also noted that the Zn codoped with Mg might not act as a scattering source for transport. However, this needs further study.

From the high resolution x-ray diffraction (HRXRD) measurement as shown in Figs. 3(a) and 3(b), both (002) and (102) HRXRD full width at half maximum (FWHM) values are broadened by increasing Cp_2Mg flow rates but not DEZn flow rates. It seems that the Zn codoping with Mg decreases the FWHM values for the (102) plane compared to Mg-doped only. This is confirmed by transmission electron microscopy (TEM) images of Figs. 3(c) and 3(d). The total dislocation densities estimated by TEM are $1 \times 10^9 \text{ cm}^{-2}$ and $2.5 \times 10^8 \text{ cm}^{-2}$ for Mg-doped only and Mg-Zn codoped GaN films, respectively. So we can conclude that the incorporation of Zn atoms with Mg is the method obtaining high conducting p -type GaN film without deterioration of the structural qualities of GaN films. It is considered that Zn might remove some dislocations by acting as a gettering dopant.¹⁰

In order to compare ohmic contact properties for Mg-doped ($6 \times 10^{17} \text{ cm}^{-3}$) only and Mg-Zn codoped ($8.5 \times 10^{17} \text{ cm}^{-3}$) p -GaN films, we performed transmission line method (TLM) with ring contact geometry with outer ring radius of $200 \mu\text{m}$ and gap spacings ($5\text{--}45 \mu\text{m}$). The surface of p -type GaN specimens was treated using aqua regia,¹¹ followed by the deposition of Pd(150 \AA)/Au(1400 \AA) ohmic metals under a vacuum condition of 10^{-5} Torr . After the metal deposition, the photoresist was lifted off. Current-voltage (I - V) characteristics of the prepared samples were estimated through HP 4155 parameter analyzer.

Figure 4(a) shows the I - V characteristics for both the Mg-doped only and the Mg-Zn codoped GaN samples, measured between the ohmic pads with a spacing of $5 \mu\text{m}$. The

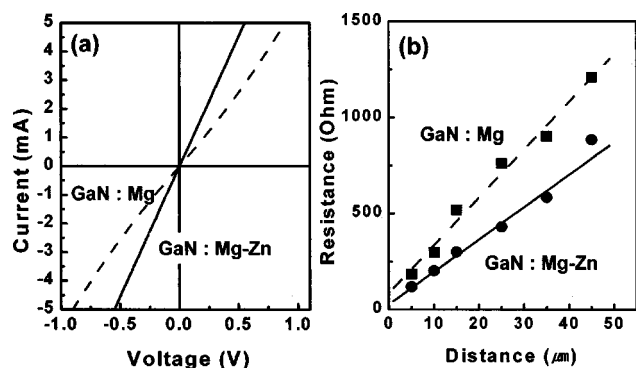


FIG. 4. (a) Comparison of the I - V characteristics measured between the contact pads with a gap spacing of $5 \mu\text{m}$ for Mg-doped only (dashed line) and Mg-Zn codoped p -type GaN films (solid line) and (b) variation of resistance as a function of gap spacing for the Mg-doped only (solid square) and Mg-Zn codoped (solid circle) p -type GaN films. Solid and dashed lines in (b) are linear fits of experimental data.

I - V curve obtained is nonlinear for the Mg-doped only sample, but linear for the Mg-Zn codoped sample over the whole range of voltages. The specific contact resistivities with correction factors¹² taken from the gradients and intercepts in the Fig. 4(b) are determined to be $1.9 \times 10^{-3} \Omega \text{cm}^2$ for the Mg-doped only sample and $5.0 \times 10^{-4} \Omega \text{cm}^2$ for the Mg-Zn codoped sample. Note that contact resistivity decreases by one order of magnitude by the codoping of Zn with Mg. Therefore, the Mg-Zn codoped GaN layer is expected to act as a good contact layer in device structure.

In conclusion, we demonstrated that, using Mg-Zn codoping, p -GaN showing low electrical resistivity ($0.7 \Omega \text{cm}$) and high hole concentration ($8.5 \times 10^{17} \text{cm}^{-3}$) were grown without the degradation of structural quality of the

film. The enhancement of electrical conducting characteristics in Mg-Zn codoping sample might be attributed to the increase of Mg activation ratio due to the reduction of hydrogen solubility. In addition, it seems that the codoping of Zn with Mg acts like a gettering treatment removing dislocations. The specific contact resistance for Mg-Zn codoped GaN film measured by TLM is $5.0 \times 10^{-4} \Omega \text{cm}^2$, which is lower value by one order of magnitude than that for Mg-doped only GaN film ($1.9 \times 10^{-3} \Omega \text{cm}^2$).

This work was partially supported by the MOST of Korea and the BK21 program of the Ministry of Education of Korea.

- ¹A. Saxler, W. C. Mitchel, P. Kung, and M. Razeghi, *Appl. Phys. Lett.* **74**, 2023 (1999).
- ²P. Kozodoy, M. Hansen, S. P. DenBaars, and U. Mishra, *Appl. Phys. Lett.* **74**, 3681 (1999).
- ³T. Yamamoto and H. K. Yoshida, *Jpn. J. Appl. Phys., Part 2* **36**, L180 (1997).
- ⁴O. Brandt, H. Yang, H. Kostial, and K. H. Ploog, *Appl. Phys. Lett.* **69**, 2707 (1996).
- ⁵K. S. Kim, G. M. Yang, and H. J. Lee, *Solid-State Electron.* **43**, 1807 (1999).
- ⁶H. Amano, K. Hiramatsu, M. Kito, N. Sawaki, and I. Akasaki, *J. Cryst. Growth* **93**, 79 (1988).
- ⁷B. Monemar, O. Lagerstedt, and H. P. Gislason, *J. Appl. Phys.* **51**, 625 (1980).
- ⁸K. S. Kim, C. S. Oh, K. J. Lee, G. M. Yang, C.-H. Hong, K. Y. Lim, A. Yoshikawa, and H. J. Lee, *J. Appl. Phys.* **85**, 8441 (1999).
- ⁹S. Nakamura, N. Iwasa, M. Senoh, and T. Mukai, *Jpn. J. Appl. Phys., Part 1* **31**, 1258 (1992).
- ¹⁰I. Ohbu, M. Ishino, and T. Mozume, *Appl. Phys. Lett.* **54**, 396 (1989).
- ¹¹J. K. Kim, J.-L. Lee, J. W. Lee, H. E. Shin, Y. J. Park, and T. Kim, *Appl. Phys. Lett.* **73**, 2953 (1998).
- ¹²L. F. Lester, J. M. Brown, J. C. Ramer, L. Zhang, S. D. Hersee, and J. C. Zolper, *Appl. Phys. Lett.* **69**, 2737 (1996).